

Mercury(II) 2-Aminoethanethiolate Clusters: Intramolecular Transformations and Mechanisms

Mohan S. Bharara, Sean Parkin, and David A. Atwood*

Department of Chemistry, University of Kentucky, Lexington, Kentucky 40506-006

Received May 18, 2006

The combination of HgF_2 and 2-aminoethanethiol (AET, with some AET·HCl present) yielded a cyclic tetranuclear thiolate, $[\text{Hg}_4\text{Cl}_4(\text{SCH}_2\text{CH}_2\text{NH}_2)_4]$ (**1**), with alternating Hg and S atoms. The Cl from the reaction mixture led to the formation of Hg–Cl bonds with no Hg–F in the final product. In contrast, a similar reaction with HgBr_2 yielded a nonanuclear cluster, $[\text{Hg}_9\text{Br}_{15}(\text{SCH}_2\text{CH}_2\text{NH}_3)_{15}]^{3+}$ (**2**), and the disulfide salt $\{[\text{HgBr}_4][(\text{NH}_3\text{CH}_2\text{CH}_2\text{S}^-)_2]\}$ (**3**). Despite similar reactions, the AET groups in **2** are protonated compared to the nonprotonated amine groups in **1**, which allows the ligand to chelate the Hg atom in the latter compound. The reaction with HgI_2 yielded a cyclic tetranuclear compound, $[\text{Hg}_4\text{I}_6(\text{SCH}_2\text{CH}_2\text{NH}_2)_2(\text{SCH}_2\text{CH}_2\text{NH}_3)_2](\text{H}_2\text{O}/\text{EtOH})$ (**4**), containing protonated and nonprotonated AET groups. Compound **4** at room temperature irreversibly rearranges to $[\text{Hg}_4\text{I}_4(\text{SCH}_2\text{CH}_2\text{NH}_2)_4]$ (**5**), which is isostructural to **1**. A systematic pathway for the formation of **1** along with the intramolecular conversion of **4** to **5** is proposed. These compounds demonstrate that very diverse Hg–S compounds form under similar reaction conditions.

Introduction

Mercury thiolates have received much attention in the last few decades because of their importance in biological Hg toxicity. Mercury thiolates have been implicated in the detoxification of Hg by metallothioneins,¹ DNA binding proteins,² and mercury reductase.³ Homoleptic mercury(II) thiolates adopt discrete molecular as well as polymeric structures with bridging S atoms.⁴ On the other hand, heteroleptic mercury(II) thiolates usually adopt polymeric structures containing bridging S atoms and halides.^{5,6} However, higher nuclearity heteroleptic mercury(II) thiolates are fairly common and include $(\text{Ph}_4\text{P})[(\mu\text{-SEt})_5(\mu\text{-Br})(\text{HgBr}_4)_4]$, $(\text{Et}_4\text{N})_2[(\mu\text{-I})(\mu\text{-SPR}^n)(\text{HgI}_2)_2]$, $(\text{Bu}^n_4\text{N})_2[\text{Hg}_4(\text{SR})_6\text{X}_4]$ (R = SEt, SPRⁿ), $[\text{Hg}_4\{\text{S}(\text{CH}_2)_2\text{N}(\text{CH}_3)_2\}_4\text{X}_4]$, and $[\text{Hg}_7(\text{SC}_6\text{H}_{11})_{12}\text{X}_2]$, where X = Cl, Br, or I.^{6–8} The structures of heteroleptic

mercury(II) thiolate clusters are usually independent of the halide present; however, the geometry around Hg is affected by the type of halide.^{6,9–12} For instance, the deviation from the tetrahedral geometry in $[\text{Hg}(\text{SR})_2\text{X}_2]$ is more pronounced for Cl than for Br and I, which has been attributed to a vibronic coupling mechanism with d-orbital involvement.¹³ The deformation is more evident in the Cl than the I derivatives because of the smaller difference in donor strength between S and Cl.

Despite the strong bonds between Hg and S, mercury(II) thiolates are typically labile and undergo ligand exchange, which is more pronounced in low-(two- and three-)coordinate compounds.¹⁴ Intra- and intermolecular exchange leads to the formation of complicated structures because the energy barrier for the exchange is low and often influenced by the nature of the solvent and the counterions.⁴ Intermolecular

* To whom correspondence should be addressed. E-mail: datwood@uky.edu.

- (1) Henkel, G.; Krebs, B. *Chem. Rev.* **2004**, *104*, 801.
- (2) Dance, I. G. *Polyhedron* **1986**, *5*, 1037.
- (3) Blower, P. J.; Dilworth, J. R. *Coord. Chem. Rev.* **1987**, *76*, 121.
- (4) Wright, J. G.; Natan, M. J.; MacDonnell, F. M.; Ralston, D. M.; O'Halloran, T. V. *Prog. Inorg. Chem.* **1990**, *29*, 323 and references cited therein.
- (5) Biscarini, P.; Foresti, E.; Paradella, G. *J. Chem. Soc., Dalton Trans.* **1984**, 953.
- (6) Alsina, T.; Clegg, W.; Fraser, K. A.; Sola, J. *J. Chem. Soc., Dalton Trans.* **1992**, 1393.
- (7) Casals, I.; Gonzalez-Duarte, P.; Sola, J.; Miravittles, C.; Molins, E. *Polyhedron* **1988**, *24*, 2509.
- (8) Dean, P. A.; Jagade, J. V.; Wu, Y. *Inorg. Chem.* **1994**, *33*, 2180.

- (9) Bermejo, E.; Castineiras, A.; Garcia, I.; West, D. X. *Polyhedron* **2003**, *22*, 1147.
- (10) Bell, N. A.; Coles, S. J.; Constable, C. P.; Hibbs, D. E.; Hursthouse, M. B.; Mansor, R.; Raper, E. S.; Sammon, C. *Inorg. Chim. Acta* **2001**, *323*, 69.
- (11) Bell, N. A.; Branston, T. N.; Clegg, W.; Creighton, J. R.; Cucurull-Sanchez, L.; Elsegood, R. J. M.; Raper, E. S. *Inorg. Chim. Acta* **2000**, *303*, 220 and references cited therein.
- (12) Stalhandske, C. M. V.; Persson, I.; Sandstrom, M.; Aberg, M. *Inorg. Chem.* **1997**, *36*, 4945.
- (13) Bersuker, I. B. *Electronic Structure and Properties of Transition Metal Compounds*; Wiley-interscience: New York, 1996.
- (14) Cheesman, B. V.; Arnold, A. P.; Rabenstein, D. L. *J. Am. Chem. Soc.* **1988**, *110*, 6359.

exchange induced by the addition of an external reagent or a change in the reaction conditions has been reported for few heteroleptic mercury(II) thiolates. For instance, the addition of excess Na_2S_2 to trinuclear $[\text{Ph}_4\text{P}]_2[\text{Hg}_3(\text{SCH}_2\text{CH}_2\text{S})_4]$ yields polymeric $\{[\text{Ph}_4\text{P}][[\text{Hg}_2(\text{SCH}_2\text{CH}_2\text{S})]\}_n$.¹⁵ Similarly, polymeric $\{\text{HgCl}_2[\text{SCH}_2\text{CH}(\text{NH}_3)\text{COOH}]\}$ in hot water rearranges to the linear bithiolate $\{\text{Hg}[\text{SCH}_2\text{CH}(\text{NH}_3)\text{COO}][\text{SCH}_2\text{CH}(\text{NH}_3)\text{COOH}]^+\}$, most probably by dissociation followed by rearrangement.¹⁶

Here we report the syntheses of mercury(II) thiolates containing an S/N ligand and proposed mechanistic pathways for the intramolecular ligand exchanges observed in the compounds. Because of the structural similarity between AET and L-cysteine, this exchange might be of importance in understanding how $\text{Hg}^{\text{II}}-\text{L}$ -cysteine bonds are made and broken in biological systems. Also, the exchange might be useful in understanding the conversion of heteroleptic mercury(II) thiolates (RSHgX) to homoleptic mercury(II) thiolates $[\text{Hg}(\text{SR})_2]$ in biological systems.

Experimental Section

General Procedure. All reactions were carried out at room temperature in deionized water under N_2 . The reagents 2-aminoethanethiol hydrochloride (TCI America), HgF_2 (Aldrich), HgBr_2 (Mallinckrodt), and HgI_2 (Alfa Aesar) were used as received. 2-Aminoethanethiol (AET) was obtained by stirring an equivalent amount of 2-aminoethanethiol hydrochloride and NaOH in methanol followed by filtration to remove NaCl. ^1H and ^{13}C NMR data were obtained with a JEOL-GSX 270 instrument operating at 200 MHz using dimethyl sulfoxide (DMSO)- d_6 as a solvent and tetramethylsilane as the reference. The $^{199}\text{Hg}\{^1\text{H}\}$ NMR spectra of **1** and **4** (0.05–0.1 M) in DMSO- d_6 were collected at 25 °C on a Varian INOV 400-MHz instrument with a 4-Nucleus Autoswitchable 5-mm probe, referenced to 1 M HgCl_2 in DMSO at -1500 ppm, and checked against external 0.1 M $\text{Hg}(\text{ClO}_4)_2$ in D_2O (-2250 ppm).^{17–19} The IR data were recorded as KBr pellets on a Mattson Galaxy 5200 FT-IR instrument between 400 and 4000 cm^{-1} . Raman spectroscopy of the solid samples were obtained on a Nicolet FT-Raman 906 spectrometer ESP between 100 and 800 cm^{-1} in the Center for Applied Energy Research at the University of Kentucky. Mass spectral data were obtained at the University of Kentucky Mass Spectrometry Facility. Elemental analysis was performed by Robertson Midrolit Laboratories, Madison, NJ.

X-ray Crystallography. Crystals of **1** were obtained in good yield either by recrystallization of the precipitate from water or by slow evaporation of the supernatant. Crystals of **2** were obtained from the recrystallization of the precipitate from hot water; however, the supernatant at room temperature yielded X-ray-quality crystals of **3**. X-ray-quality crystals of **4** were obtained from the supernatant at 4 °C. X-ray diffraction data for **1** and **3** were collected at 90 K on a Nonius Kappa CCD diffractometer unit using $\text{Mo K}\alpha$ radiation and those for **4** were collected at 90 K on a Bruker-Nonius $\times 8$ Proteum diffractometer unit using $\text{Cu K}\alpha$ radiation, both from regular-shaped crystals mounted in Paratone-N oil on glass fibers. The initial cell parameters were obtained using DENZO²⁰ from 1°

frames and were refined with a least-squares scheme using all data-collection frames (SCALEPACK).²⁰ The structures were solved by direct methods (SHELXL97)²¹ and completed by difference Fourier methods (SHELXL97).²¹ Refinement was performed against F^2 by weighted full-matrix least squares, and empirical absorption corrections (SADABS²¹) were applied. H atoms were placed at calculated positions using suitable riding models with isotropic displacement parameters derived from their carrier atoms. Non-H atoms were refined with anisotropic displacement parameters. Atomic scattering factors were taken from *International Tables for Crystallography Volume C*.²² Crystal data, selected bond distances and angles, are provided in Tables 1–3.

Synthesis of 2-Aminoethanethiol (AET). To a stirring solution of 2-aminoethanethiol hydrochloride (12 mmol, 1.36 g) in methanol was added NaOH (12 mmol, 0.48 g), and the resulting solution was stirred for 2–3 h. The white precipitate of NaCl was filtered, and the resulting clear solution was vacuum-dried to obtain AET. In the synthesis of **1**, AET still contained Cl.

Synthesis of $[\text{Hg}_4\text{Cl}_4(\text{SCH}_2\text{CH}_2\text{NH}_2)_4]$ (1**).** AET (10 mmol, 0.77 g) was dissolved in deionized water (70 mL) under a flow of N_2 ; to this was added HgF_2 (5 mmol, 1.19 g) as a suspension in methanol (30 mL), and the resulting solution was stirred for 48 h. The resulting white precipitate was filtered, washed with deionized water and methanol, and dried. The filtrate at room temperature yielded X-ray-quality crystals. Colorless crystals could also be obtained from the recrystallization of precipitate from water. Yield (crystals + ppt): 0.66 g (10%). Mp: 170–172 °C (dec). ^1H NMR (DMSO- d_6 , 200 MHz, ppm): δ 2.91–2.93 (m, 4H, $\text{NCH}_2\text{CH}_2\text{S}$), 3.82 (b, 2H, NH_2). ^{13}C NMR (DMSO- d_6 , 200 MHz, ppm): δ 30.9 (CH_2S), 41.8 (CH_2N). IR/Raman (KBr, ν/cm^{-1}): 3444, 3242, 3157, 2966, 1627, 1592, 1421, 1386, 1021, 916, 648, 483, 345, 280, 225. MS (EI, +ve): 311 ($[\text{M}/4]^+$), 279 ($[\text{311} - \text{S}]^+$), 265 ($[\text{279} - \text{CH}_2]^+$), 251 ($[\text{265} - \text{CH}_2]^+$), 235 ($[\text{251} - \text{NH}_2]^+$), 200 ($[\text{235} - \text{Cl}]^+$), 76 ($[\text{SCH}_2\text{CH}_2\text{NH}_2]^+$). Anal. Calcd for $[\text{Hg}_4\text{Cl}_4(\text{SCH}_2\text{CH}_2\text{NH}_2)_4]$: C, 7.694; H, 1.937; N, 4.480. Found: C, 7.793; H, 1.986; N, 4.450.

Synthesis of $\{[\text{HgBr}_4][(\text{NH}_2\text{CH}_2\text{CH}_2\text{S})_2]\}$ (3**).** AET (10 mmol, 0.77 g) was dissolved in deionized water (70 mL) under a flow of N_2 ; to this was added HgBr_2 (5 mmol, 1.8 g) as a suspension in methanol (30 mL), and the resulting solution was stirred for 48 h. The resulting white precipitate was filtered, washed with deionized water and methanol, and dried (1.74 g). Recrystallization of the precipitate from water yielded crystals of $[\text{Hg}_9\text{Br}_{15}(\text{SCH}_2\text{CH}_2\text{NH}_2)_{15}]^{3+}$ (**2**).²³ Colorless crystals of **3** were obtained from the supernatant at room temperature. Crystalline yield: 0.37 g (10%). Mp: 220–220 °C (dec). ^1H NMR (DMSO- d_6 , 200 MHz, ppm): δ 2.99 (t, 2H, CH_2S), 3.10 (t, 2H, CH_2N), 7.92 (b, 3H, NH_2). ^{13}C NMR (DMSO- d_6 , 200 MHz, ppm): δ 33.9 (CH_2S), 42.9 (CH_2N). IR/Raman (KBr, ν/cm^{-1}): 3440, 3009, 2718, 1634, 1588, 1475, 1456, 1382, 1091, 885, 819, 765, 65, 466, 165. Anal. Calcd for $\text{HgBr}_4\text{C}_4\text{H}_{14}\text{N}_2\text{S}_2$: C, 7.122; H, 2.092; N, 4.153. Found: C, 7.099; H, 2.046; N, 4.145.

Synthesis of $[\text{Hg}_4\text{I}_6(\text{SCH}_2\text{CH}_2\text{NH}_2)_2(\text{SCH}_2\text{CH}_2\text{NH}_3)_2](\text{H}_2\text{O}/\text{EtOH})$ (4**).** To a stirring solution of AET (10 mmol, 0.77 g) in deionized water (70 mL) was HgI_2 (5 mmol, 2.27 g) dissolved in ethanol (30 mL), and the resulting solution was stirred for 3 days.

(15) Henkel, G.; Betz, P.; Krebs, B. *Chem. Commun.* **1985**, 1498.

(16) Taylor, N. J.; Carty, A. J. *J. Am. Chem. Soc.* **1977**, *99*, 6143.

(17) Sens, M. A.; Wilson, N. K.; Ellis, P. D.; Odon, J. D. *J. Magn. Reson.* **1975**, *19*, 323.

(18) Al-Showiman, S. S. *Inorg. Chim. Acta* **1988**, *141*, 263.

(19) Pregosin, P. S. *Transition Metal Nuclear Magnetic Resonances*; Wiley: New York, 1991.

(20) Otwinowski, Z.; Moinor, W. *Methods Enzymol.* **1997**, *276*, 307.

(21) Sheldrick, G. M. *SADABS—An empirical adsorption correction program*; Bruker Analytical X-ray Systems: Madison, WI, 1996.

(22) *International Tables for Crystallography Volume C*; Kluwer Academic Publishers: Dordrecht, The Netherlands, 1992.

(23) Bharara, M. S.; Bui, T. H.; Parkin, S.; Atwood, D. A. *Inorg. Chem.* **2005**, *44*, 5753.

Table 1. Crystal Data for Compounds **1**, **3**, and **4**

data	1	3	4
empirical formula	C ₄ H ₁₂ Cl ₂ Hg ₂ N ₂ S ₂	C _{2.67} H _{10.67} Br _{2.67} Hg _{0.67} N _{1.33} O _{0.67} S _{1.33}	C _{5.28} H _{16.2} Hg ₂ I ₃ N ₂ OS ₂
fw	624.36	461.69	969.76
<i>T</i> (K)	90.0(2)	90.0(2)	90.0(2)
wavelength (Å)	0.710 73	0.710 73	1.541 78
cryst syst	monoclinic	monoclinic	monoclinic
space group	<i>P</i> 2 ₁ / <i>c</i>	<i>P</i> 2 ₁ / <i>c</i>	<i>P</i> 2 ₁ / <i>c</i>
<i>a</i> (Å)	7.9463(10)	6.3250(13)	12.3749(2)
<i>b</i> (Å)	16.2097(2)	12.381(3)	8.1190(2)
<i>c</i> (Å)	9.77580(10)	10.112(2)	17.9245(4)
α (deg)	90.0	90.0	90.0
β (deg)	109.844(10)	101.16(3)	105.578(10)
γ (deg)	90.0	90.0	90.0
<i>V</i> (Å ³)	1184.42(2)	776.9(3)	1737.42(6)
<i>Z</i>	4	3	4
density calcd (mg/m ³)	3.501	2.961	3.705
abs coeff (mm ⁻¹)	26.650	20.439	75.182
<i>F</i> (000)	1104	628	1684
cryst size (mm ³)	0.10 × 0.10 × 0.05	0.10 × 0.10 × 0.05	0.05 × 0.02 × 0.01
reflns collected	5311	17 635	22 510
indep reflns	2717 (<i>R</i> _{int} = 0.0274)	3546 (<i>R</i> _{int} = 0.0605)	3128 (<i>R</i> _{int} = 0.0638)
refinement method	full-matrix least squares on <i>F</i> ²	full-matrix least squares on <i>F</i> ²	full-matrix least squares on <i>F</i> ²
GOF on <i>F</i> ²	1.066	1.055	1.059
final <i>R</i> indices [<i>I</i> > 2σ(<i>I</i>)]	<i>R</i> 1 = 0.0247 w <i>R</i> 2 = 0.0553	<i>R</i> 1 = 0.0345 w <i>R</i> 2 = 0.0660	<i>R</i> 1 = 0.0366 w <i>R</i> 2 = 0.0912
<i>R</i> indices (all data)	<i>R</i> 1 = 0.0316 w <i>R</i> 2 = 0.0575	<i>R</i> 1 = 0.0463 w <i>R</i> 2 = 0.0697	<i>R</i> 1 = 0.0397 w <i>R</i> 2 = 0.0933
extinction coeff	0.00030(7)	0.0015(2)	0.000128(17)
largest diff peak and hole (e/Å ³)	1.723 and -1.343	1.805 and -1.727	3.665 and -3.134

Table 2. Selected Bond Distances (Å) and Angles (deg) for **1**^a

Hg1–S1	2.5535(1)	Hg1–S2	2.4082(1)
Hg2–S1#1	2.4121(1)	Hg2–S2	2.4679(1)
Hg1–N1	2.293(5)	Hg1–Cl1	2.6565(1)
Hg2–N2	2.449(5)	Hg2–Cl2	2.6862(1)
Hg1–S2–Hg2	102.50(5)	Hg2–S1–Hg1#1	98.48(5)
S1–Hg1–S2	132.11(5)	S1–Hg1–N1	82.34(1)
S2–Hg1–N1	138.76(1)	S1–Hg1–Cl1	98.42(5)
S2–Hg1–Cl1	101.66(5)	N1–Hg1–Cl1	92.61(1)
S1–Hg2–N2#1	120.12(1)	S1–Hg2–S2#1	146.18(5)
N2–Hg2–S2	81.07(12)	S1–Hg2–Cl2#1	103.82(5)
N2–Hg2–Cl2	86.77(12)	S2–Hg2–Cl2	103.38(5)

^a #1 = -*x* + 1, *n* - *y*, -*z* + 1.**Table 3.** Bond Distance (Å) and Angles (deg) for **4**^a

Hg1–S2	2.498(2)	Hg1–S1	2.519(2)
Hg2–S1	2.468(2)	Hg2–S2#1	2.486(2)
Hg2–N2#1	2.391(8)	N2–Hg2#1	2.391(8)
Hg1–I1	2.8130(7)	Hg1–I2	2.8613(7)
Hg2–I3	2.8078(7)	S2#1–Hg2	2.486(2)
S2–Hg1–S1	117.34(7)	S2–Hg1–I1	110.89(5)
S1–Hg1–I1	110.51(5)	S2–Hg1–I2	107.89(5)
N2–Hg2–S1	113.5(2)	N2–Hg2–S2	82.37(19)
S1–Hg2–S2#1	135.91(7)	Hg2–S1–Hg1	103.12(8)
S1–Hg1–I2	108.09(5)	S1–Hg2–I3	108.71(5)

^a #1 = -*x*, -*y* + 1, -*z*.

The light-yellow precipitate was removed by filtration, washed with water and ethanol, and vacuum-dried. The supernatant cooled to 4 °C yielded light-yellow crystals. Yield (crystals + ppt): 3.2 g (68%). Mp: 188–190 °C (dec). ¹H NMR (DMSO-*d*₆, 200 MHz, ppm): δ 2.94 (b, 4H, NCH₂CH₂S), 3.58 (b, 2H, NH₂). ¹³C NMR (DMSO-*d*₆, 200 MHz, ppm): δ 32.4 (CH₂S), 41.4 (CH₂N). IR/Raman (KBr, ν/cm⁻¹): 3445, 3164, 2831, 1601, 1555, 1364, 1266, 1153, 1018, 935, 630, 453, 345, 289, 220, 163, 129. MS (EI, +ve): 679 ([Hg₂C₄H₁₃N₂S₂I₂]⁺), 351 ([HgC₄H₁₃N₂S₂]⁺), 336 ([351 - CH₂]⁺), 326 ([336 - CH₂]⁺), 278 ([Hg(SCH₂CH₂NH₂)⁺], 202 ([Hg]⁺), 77 ([SCH₂CH₂NH₃]⁺). Anal. Calcd for [Hg₄I₆S₄C₁₀H₃₁N₄O₂]:

C, 6.218; H, 1.617; N, 2.900. Found: C, 6.199; H, 1.596; N, 3.001 (crystals) and C, 6.189; H, 1.560; N, 3.017 (precipitate).

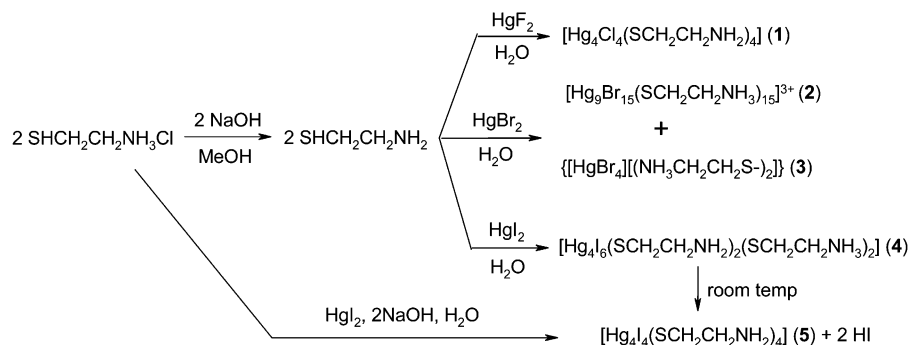
Result and Discussion

The combination of AET with HgF₂ in a mixture of deionized water and methanol (70:30) yielded **1** in low yield, where the Cl originated as an impurity in AET (AET contained a small amount of AET·HCl). A similar reaction with HgBr₂ precipitates a nonanuclear compound, [Hg₉Br₁₅(SCH₂CH₂NH₃)₁₅]³⁺ (**2**), which was reported previously.²³ However, the supernatant at room temperature yielded colorless crystals of **3**. A similar reaction with HgI₂ in a mixture of water and ethanol (70:30) yielded a light-yellow precipitate of **4**. The light-yellow crystals of **4**, obtained from the supernatant at 4 °C, irreversibly yielded [Hg₄I₈(SCH₂CH₂NH₂)₄] (**5**) at room temperature. Compound **5** could also be obtained from the direct combination of HgI₂ and AET·HCl in the presence of an equivalent amount of NaOH.²⁴ The conversion of **4** to **5** at room temperature did not occur in DMSO as shown in ¹⁹⁹Hg NMR. The conversion of **5** to **4** is not observed in either water or DMSO. The reactions are summarized in Scheme 1.

Crystallographic data for structural analysis of compounds **1**, **3**, and **4** have been deposited with the Cambridge Crystallographic Data Center as CCDC Nos. 606889, 606890, and 606891, respectively. Copies of this information may be obtained free of charge from The Director, CCDC, 12 Union Road, Cambridge CB2 1EZ, U.K. (phone +44 1223 336408; fax +44 1223 336033).

Spectroscopy. The ¹H and ¹³C NMR spectra for compounds **1**, **3**, and **4** indicate symmetrical solution structures.

(24) Bharara, M. S.; Parkin, S.; Atwood, D. A. *Inorg. Chem.* **2006**, *45*, 2112.

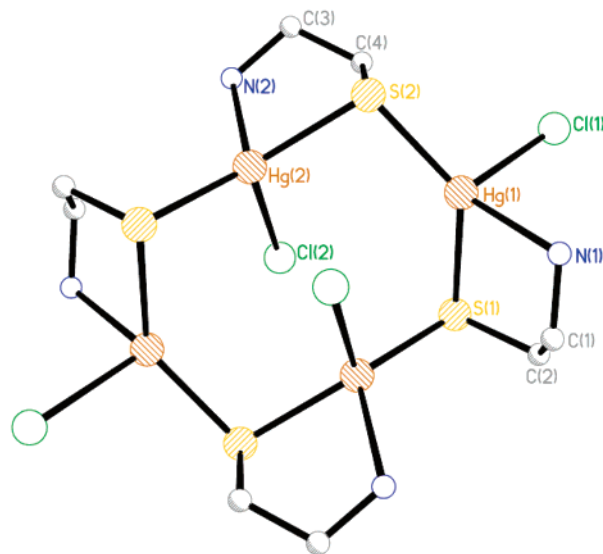
Scheme 1. Reaction Scheme Showing the Syntheses of Compounds 1–5

In the ^1H NMR, the peaks for the SCH_2 protons in **1** and **4** show slight downfield shifts from the free ligand (2.69 ppm) due to the presence of the Hg-S bonds. Despite the Hg-N bonds, the NCH_2 protons do not show significant shifts in **1** and **4**. For **3**, the peak for the ammonium group is observed at 8 ppm. In the ^{13}C NMR for **1**, the peak due to C-S is observed at 29 ppm, similar to that observed in **5**. However, in **4**, this peak is slightly deshielded and appears at 32 ppm. The peak for C-N in both **1** and **4** appears at 41 ppm and is comparable to that of **5** (42 ppm). In the ^{199}Hg NMR spectrum of **1**, a single broad peak is observed at -704 ppm, indicating a tetrahedral coordination environment around Hg. The coupling between Hg and N atoms is responsible for the broadness of the peak. A similar broad peak is observed in **5** (-642 ppm), which is similar to that of other mercury(II) thiolates containing Hg-N bonds such as $[\text{Hg}(\text{SCH}_2\text{CH}_2\text{NH}_2)_2]$ (-659 ppm).^{24,25} The ^{199}Hg NMR for **4** in $\text{DMSO-}d_6$ shows two distinct peaks at -2983 and -1928 ppm, which could be assigned to $[\text{HgI}_2\text{S}_2]$ and $[\text{HgIS}_2\text{N}]$ coordination environments, respectively. The deshielding present in the first peak is due to the presence of two Hg-I bonds (free $\text{HgI}_2 = -3435$ ppm).²⁶ Despite a $[\text{HgIS}_2\text{N}]$ environment similar to that in **5**, a broad peak around -600 ppm is not observed in **4**. Such upfield shielding in $[\text{HgIS}_2\text{N}]$ could be attributed to the strained octagonal ring in **4** compared to **5** (Figure 4).

The IR spectra for **1** and **4** are quite similar, with the absence of the $-\text{SH}$ peak around 2500 cm^{-1} . A weak peak observed at 600 cm^{-1} in **3** indicates the presence of the disulfide group. In **1** and **4**, peaks in the range $3000\text{--}3400 \text{ cm}^{-1}$ could be assigned to symmetric and asymmetric $-\text{NH}_2$ stretches. In **3**, peaks around 2900 and $1400\text{--}1500 \text{ cm}^{-1}$ could be assigned to symmetric $-\text{NH}_3$ stretches and symmetric deformation and degenerate deformation modes, respectively. Similar peaks are also observed for **4** because of the presence of both $-\text{NH}_2$ and $-\text{NH}_3$ groups. In the Raman spectra, symmetric and asymmetric stretching frequencies for Hg-S are observed around 250 and 340 cm^{-1} for **1** and 289 and 345 cm^{-1} for **4** (see the Supporting Information). In both **1** and **4**, the stretch due to Hg-N could be assigned to peaks around 483 and 460 cm^{-1} , respectively, and are in the range observed for mercury(II) thiolates with

Hg-N bonds ($400\text{--}700 \text{ cm}^{-1}$).^{24,27,28} The stretch around 220 cm^{-1} in **1** could be assigned to the Hg-Cl bond, which is in accord with the stretch observed in mercury(II) thiolates with terminal Cl atoms ($220\text{--}235 \text{ cm}^{-1}$).^{12,23,28–30} In **3**, the stretch due to terminal Hg-Br appears at 165 cm^{-1} , close to that observed in $[\text{Hg}_2\text{Br}_6]^{2-}$ (150 cm^{-1}).³¹ The terminal Hg-I frequency for **4** can be assigned to the peak observed around 129 cm^{-1} , which is similar to that observed in **5** (127 cm^{-1}) as well as frequencies reported in the literature.^{12,24,32}

Structures. Compound **1** is tetranuclear with an eight-membered ring consisting of alternating Hg and S atoms (Figure 1). The distorted tetrahedral Hg coordination consists

**Figure 1.** Structure of **1**. H atoms are not shown for clarity.

of S, N, and Cl atoms, with the neighboring Cl atoms present above and below the plane defined by the Hg and S atoms. The Hg-S distances in the S/N chelate ($\text{Hg1-S1} = 2.554$

(25) Fleischer, H.; Dienes, Y.; Mathiasch, B.; Schmitt, V.; Schollmeyer, D. *Inorg. Chem.* **2005**, *44*, 8087.

(26) Goodfellow, R. J. *Multinuclear NMR*; Plenum Press: New York, 1987.

(27) Nakamoto, K. *Infrared Spectra of Inorganic and Coordination Compounds*; Wiley: New York, 1963.

(28) Bharara, M. S.; Bui, T. H.; Parkin, S.; Atwood, D. A. *J. Chem. Soc., Dalton Trans.* **2005**, 3874 and references cited therein.

(29) Biscarini, P.; Fusina, L.; Nivelline, G. *J. Chem. Soc., Dalton Trans.* **1974**, 2140.

(30) Fleissner, G.; Kozłowski, P. M.; Vargek, M.; Bryson, J. W.; O'Halloran, T. V.; Spiro, T. G. *Inorg. Chem.* **1999**, *38*, 3523 and references cited therein.

(31) Castineiras, A.; Arquero, A.; Masaguer, J. R.; Martínez-Carrera, S.; García-Blanco, S. *Z. Anorg. Allg. Chem.* **1986**, *539*, 219.

(32) Bell, N. A.; Branston, T. N.; Clegg, W.; Parker, L.; Raper, E. S.; Constable, C. P.; Sammon, C. *Inorg. Chim. Acta* **2001**, *319*, 130.

Å and $\text{Hg2-S2} = 2.468$ Å) are longer compared to the non-chelate Hg-S bonds ($\text{Hg1-S2}'' = 2.408$ Å and $\text{Hg2-S1} = 2.412$ Å; Table 2). This is due to the strain in the five-membered ring. These distances, in general, fall in the range observed for tetrahedral mercury(II) thiolates (2.410–2.606 Å).^{5,12} However, the distances are much shorter than the corresponding distances observed in polymeric $[\text{HgCl}(\text{SCH}_2\text{CH}_2\text{NH}_2)]_n$ (**6**) (2.652 Å), which contains a similar Hg environment, namely, an S/N chelate and bridging S and terminal Cl atoms.²⁸ The shorter bonds in **1** imply a stable cyclic structure compared to the open chain observed in **6**. Compound **1** is closely related to $[\text{Hg}_4\text{Cl}_4\{\text{S}(\text{CH}_2)_2\text{NMe}_2\}_4]$ (**7**), which contains an octagonal ring and five-membered S/N chelates.³³ However, two independent Hg centers are observed in **7**, with HgS_2Cl_2 and HgS_2N_2 coordination environments. The average Hg-S distances in **7** (2.414 Å) are intermediate to those observed in **1**. In **1**, the Hg-N distance associated with Hg1 (2.293 Å) is much shorter compared to the corresponding distance associated with Hg2 (2.449 Å), indicating a stronger bond associated with Hg1. Despite similar environments, the difference in the Hg-N bonds in **1** (0.156 Å) is much larger compared to those in **6** (0.009 Å) and **7** (0.042 Å). Unsymmetrical bonds in mercury(II) thiolates are not unusual and provide overall synergic stability to the molecule.³⁴ The terminal Hg-Cl distances (2.686 and 2.656 Å) in **1** are smaller than those observed in **6** (average 2.718 Å)²⁸ but comparable to those in mercury(II) thiolates containing terminal Cl atoms (2.58–2.81 Å).^{7,16,35,36}

The S-Hg-S angles spanning Hg1 (132°) and Hg2 (146°) are in accordance with the corresponding angles observed for **6** (125 – 137°) but shorter compared to the most obtuse S-Hg-S angle observed in **7** (163°). The latter is most probably due to a symmetrical environment around Hg.³³ The S-Hg-N chelate angles spanning Hg1 and Hg2 (average 81°) are similar to those observed for **6** (81°) and **7** (82°) despite the considerable differences observed in the bond distances. The Hg-S-C angles in the chelate are similar for **1** (average 94°) and **6** (average 94°) but more narrow than that for **7** (103°), indicating a more strained five-membered ring in the previous two compounds.

Compound **2** has been described previously in detail.²³ The nonanuclear cluster consists of four independent Hg centers, namely, $\text{HgS}_2(\mu\text{-Br})_2$, $\text{HgS}_2(\mu\text{-Br})\text{Br}$, HgSBr_3 , and HgS_2Br with variable geometry around the Hg atoms. As shown in Figure 2, the structure of **3** consists of $[\text{HgBr}_4]^{2-}$ and a disulfide of two AET molecules containing ammonium groups. It is interesting to observe that the environment around Hg is distorted tetrahedral with Br-Hg-Br angles in the range 99 – 126° , rather than perfectly tetrahedral, as might have been expected. This distortion could be attributed

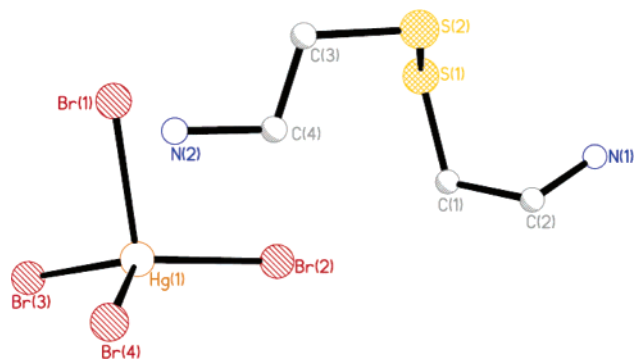


Figure 2. Asymmetric unit observed in **3**. The H atoms and water molecules are not shown for clarity.

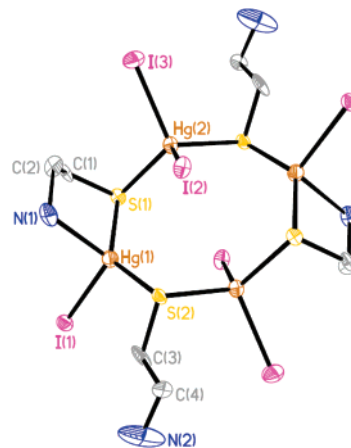


Figure 3. Crystal structure of **4**. Solvent molecules and H atoms are not shown for clarity.

to intermolecular H bonding. The individual units are connected through weak intermolecular H bonding involving N, S, Br, and O atoms. The NH-Br distances are in the range 3.293–3.556 Å and longer than those observed in **2** (3.131–3.434 Å),²³ $[\text{HgBr}_2(1,3\text{-thiazolidine-2-thione})_2]$ (3.297–3.335 Å),¹⁰ and $[[\text{HgBr}_2(1,3\text{-imidazole-2-thione})_2]$ (3.286–3.406 Å).^{37,38}

Compound **4**, a centrosymmetric tetranuclear molecule with an eight-membered ring consisting of alternating Hg and S, is similar to **1** (Figure 3). The octagonal ring is nonplanar, with the I atoms and S/N chelate present on the opposite sides of the mean plane defined by four Hg and four S atoms. Two independent Hg centers, namely, HgI_2S_2 and HgIS_2N , with distorted tetrahedral geometries are observed. The Hg-S distances in **4** are variable and depend on the coordination environment around Hg. Unsymmetrical Hg-S distances around Hg2 (2.468 and 2.498 Å) are due to the formation of the five-membered chelate. These distances are comparable to the corresponding distances in **1** but shorter than those observed in **5** (2.476 and 2.518 Å), indicating a stronger bond.²⁴ The Hg-N distance (2.391 Å) in **4** is intermediate to the corresponding distances observed in **5** (2.371 and 2.404 Å). The Hg-I distance (2.808 Å) associated with the HgIS_2N unit is longer than the corresponding distance observed in **5** (average 2.758 Å) but comparable to

(33) Casals, I.; Gonzalez-Duarte, P.; Clegg, W.; Foces-Foces, C.; Cano, F. H.; Martinez-Ripoll, M.; Gomez, M.; Solans, X. *J. Chem. Soc., Dalton Trans.* **1991**, 2511.

(34) Govindaswamy, N.; Moy, J.; Millar, M.; Koch, S. A. *Inorg. Chem.* **1992**, *31*, 5343.

(35) Cauty, A. J.; Raston, C. L.; White, A. H. *Aust. J. Chem.* **1978**, *31*, 677.

(36) Pavlovic, G.; Popovic, Z.; Soldin, Z.; Matkovic-Calogovic, D. *Acta Crystallogr., Sect. C* **2000**, *C56*, 61.

(37) Popovic, Z.; Matkovic-Calogovic, D.; Soldin, Z.; Pavlovic, G.; Davidovic, N.; Vikić-Topić, D. *Inorg. Chim. Acta* **1999**, *294*, 35.

(38) Steiner, T. *Angew. Chem., Int. Ed.* **2002**, *41*, 48.

those observed in $[\text{HgI}_x(\text{SR})_y]$ thiolates (2.72–2.78 Å).⁸ The Hg–I distances associated with the HgS_2I_2 units are unsymmetrical (average 2.837 Å) and longer compared to the sum of covalent radii of tetrahedral Hg and I (2.81 Å).³⁹ The angles associated with the HgS_2I_2 unit (107–110°) show less distortion from ideal tetrahedral geometry compared to those associated with the HgIS_2N unit (82–135°). The distortion in the HgIS_2N unit is due to the formation of the five-membered chelate. The S1–Hg2–S1' angle in **4** (136°) is more linear compared to the corresponding angle observed in **5** (123°), due to the unsymmetrical environment around Hg2.

Intermolecular Interactions. The shortest Hg–Hg interactions observed in **1** and **4** are those observed between Hg1 and Hg2 [3.782 Å (**1**) and 3.924 Å (**4**)]. These distances indicate no mercuriphilic interaction and are in the range usually observed for heteroleptic mercury(II) thiolates (3.648–3.852 Å).^{9,35,40,41} Despite having similar octagonal frameworks, the Hg–Hg interactions are variable and shorter for **1** compared to those observed in **4** and **5** (average 3.901 Å).

The individual molecules in **1**, **3**, and **4** are connected through weak intermolecular H bonding involving N and X (Cl, Br, and I), yielding a unidirectional chain (see the Supporting Information). The NH–Cl distances (average 3.4 Å) in **1** are comparable to those in **6** (average 3.4 Å) but smaller than those observed in $[\text{HgCl}_2\{\mu\text{-S}(\text{CH}_2)_3\text{NH}(\text{CH}_3)_3\}]$ (3.15 Å)⁷ and $[\text{HgCl}_2\{\text{C}_3\text{H}_4\text{N}_2\text{S}\}_2]$ (average 3.154 Å).³⁶ The NH–I (average 3.60 Å) distances in **3** are shorter compared to those observed in **5** (average 3.80 Å) but in the range observed for $[\text{HgI}_2(\text{SR})]$ compounds [SR = benzo-1,3-imidazole-2-thione (average 3.59 Å); 1-methyl-imidazoline-2(3*H*)-thione (average 3.59 Å)].¹¹ In contrast to **1**, weak NH–S interactions are observed in **3** (3.70 Å) and **4** (3.55 Å). These distances are comparable to tetrahedral mercury(II) thiolates with similar interactions (3.39–3.73 Å).^{42,43} The nonplanarity of the octagonal ring in both **1** and **4** is most probably due to the weak interactions as well as the steric effects of the halide. As shown in Figure 4, the deformation observed in the chair configuration acquired by **1** is more distinct compared to that of **4** or **5**. This is most probably due to the symmetrically packed I atoms, resulting in restricted vibrational motion in the crystal.

Mechanistic Pathways. A mechanistic pathway for the formation of **1** (Scheme 2) and **4** (Scheme 3) can be proposed similarly to that of **5**.²⁴ Because of more ionic character, HgF_2 will dissociate completely and the free Hg^{2+} reacts with AET to form a two-coordinate intermediate $[\text{Hg}(\text{S/N})]^+$. This intermediate can further combine with either F^- or a second 1 equiv of AET to form $[\text{HgF}(\text{S/N})]$ and $[\text{Hg}(\text{S/N})_2]$,

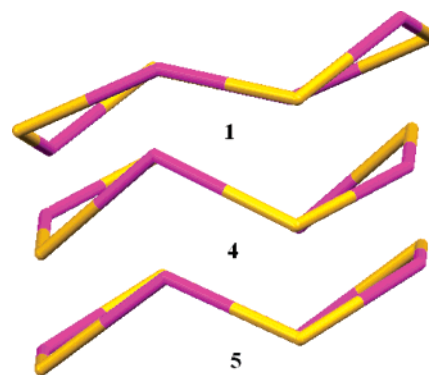
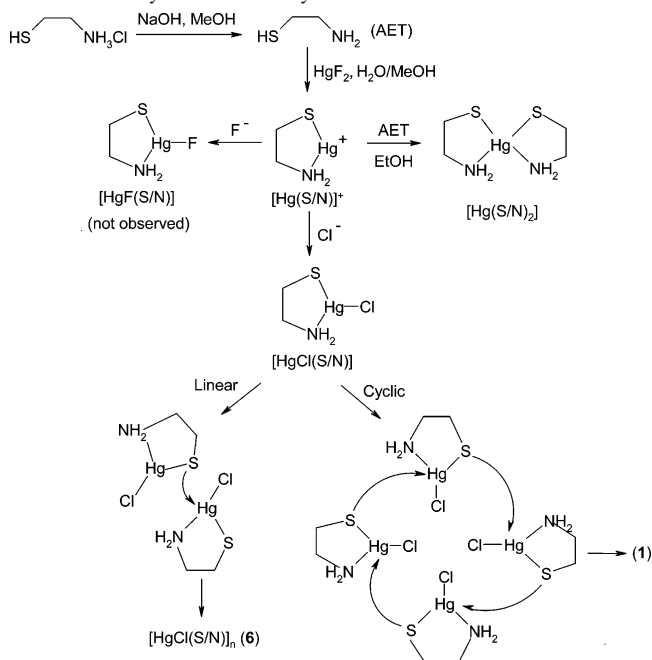


Figure 4. Relaxed chair configuration acquired by **1**, **4**, and **5**.²⁴ The alternating Hg and S atoms in the ring are not labeled for clarity.

Scheme 2. Systematic Pathway for the Formation of **1**



respectively. However, the formation of an Hg–F bond is highly unlikely because of the mismatch in soft Hg^{2+} and hard F^- ions. The formation of $[\text{Hg}(\text{S/N})_2]$ has been reported from less polar solvents without the presence of halide ions.²⁵ Hence, it can be argued that the structure adopted by a mercury(II) thiolate cluster depends on the halide present in the solution. The three-coordinate intermediate $[\text{Hg}(\text{S/N})\text{Cl}]$ is not known to exist because it is highly unstable and readily forms a four-coordinate compound. This is achieved by the formation of an additional Hg–S bond in preference to an Hg–Cl bond, which is evident from the bond energies (Hg–S = 217 kJ/mol and Hg–Cl = 100 kJ/mol). The $[\text{HgCl}(\text{S/N})]$ species can react sideways to form polymeric **6**²⁸ or rearrange to form a cyclic structure (**1**). The formation of a cyclic cluster is preferred over the linear polymeric chain to achieve overall stability, which is also evident from the shorter bridging Hg–S bonds observed in the former compound.

In the formation of **4**, the first step involves the two three-coordinate intermediates, $[\text{HgI}_2(\text{SR})]$ and $[\text{HgI}(\text{S/N})]$. This is possible because of the presence of AET as a zwitterion in solution.²⁵ The $[\text{HgI}_2\text{S}]$ intermediate has been reported

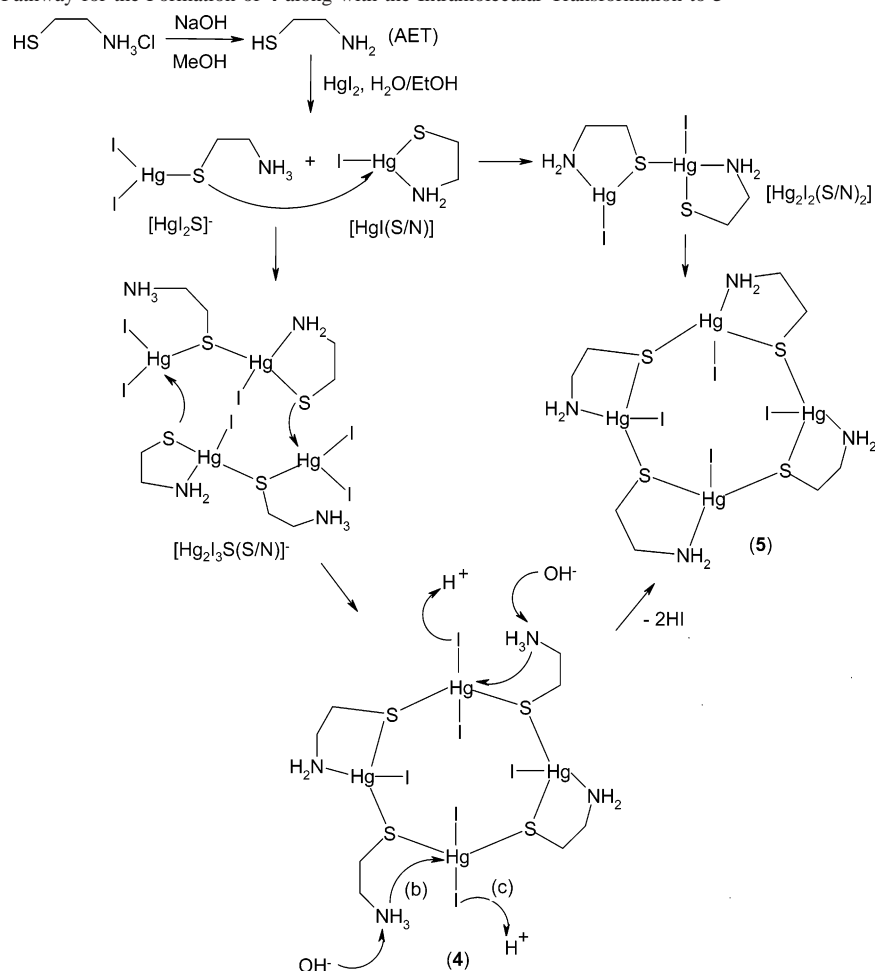
(39) Pauling, L. *The Nature of the Chemical Bonding*; Cornell University Press: Ithaca, NY, 1960.

(40) Canty, A. J.; Raston, C. L.; White, A. H. *Aust. J. Chem.* **1979**, *32*, 311.

(41) Bermejo, E.; Castineiras, A.; Garcia-Santos, I.; West, D. X. *Z. Anorg. Allg. Chem.* **2004**, *630*, 1096.

(42) Popovic, Z.; Pavlovic, G.; Soldin, Z.; Popovic, J.; Matkovic-Calogovic, D.; Rajic, M. *Struct. Chem.* **2002**, *13*, 415.

(43) Popovic, Z.; Soldin, Z.; Matkovic-Calogovic, D.; Pavlovic, G.; Rajic, M.; Giester, G. *Eur. J. Inorg. Chem.* **2002**, 171.

Scheme 3. Systematic Pathway for the Formation of **4** along with the Intramolecular Transformation to **5**

earlier for mercury(II) thiolates containing relatively large ligands such 1,3-thiazolidine-2-thione and 1,3-imidazole-2-thione.^{37,42} Similarly, $[\text{HgI}(\text{S}/\text{N})]$ intermediates have been reported in solution for mercury(II) thiolates with S/N chelates.^{44,45} The stability around the three-coordinate intermediates is achieved by forming a stable fourth bond, $\text{Hg}-\text{S}_{\text{bridging}}$, in preference to an $\text{Hg}-\text{I}$ (bond energies 217 and 35 kJ/mol, respectively), similar to that observed for $[\text{Hg}(\text{S}/\text{N})\text{Cl}]$ in **1**. This is evident from the crystal structure, where the bridging $\text{Hg}-\text{S}$ bond is shorter than the chelated $\text{Hg}-\text{S}$ bond. For the formation of **4**, the $[\text{HgI}(\text{S}/\text{N})]$ intermediate combines with the $[\text{HgI}_2\text{S}]$ intermediate to form the dinuclear species, $[\text{Hg}_2\text{I}_3\text{S}(\text{S}/\text{N})]$. However, for **5**, $[\text{HgI}(\text{S}/\text{N})]$ rearranges to form $[\text{HgI}_2(\text{S}/\text{N})_2]$ species. Both dinuclear species still contain a three-coordinate Hg center, which combines further with another dinuclear intermediate to form a tetranuclear cluster.

The intramolecular conversion of **4** to **5** can be postulated to proceed through either three- or five-coordinate intermediates, namely, $[\text{HgI}_2\text{S}_2\text{N}]^{2-}$ or $[\text{HgI}_2\text{S}_2\text{N}]^{2-}$. The H^+ in the solution removes I from the $[\text{HgI}_2\text{S}_2]$ unit to form an $[\text{HgI}_2\text{S}_2]^-$, a three-coordinate intermediate. This might be due

to the longer $\text{Hg}-\text{I}$ bond associated with the $[\text{HgI}_2\text{S}_2]$ unit compared to the $[\text{HgI}(\text{S}/\text{N})]$ unit. The $-\text{NH}_3$ groups are deprotonated to form $-\text{NH}_2$ through nucleophilic attack of OH^- , which is a better nucleophile in the presence of HI. The fourth coordination around Hg is further completed by the formation of an $\text{Hg}-\text{N}$ bond to form $[\text{HgI}_2\text{S}_2\text{N}]^{2-}$ and yield **5**. However, a free $-\text{NH}_2$ group can also form an $\text{Hg}-\text{N}$ bond and $[\text{HgI}_2\text{S}_2\text{N}]^{2-}$, a five-coordinate intermediate. In the next step the H^+ in the solution removes I from the $[\text{HgI}_2\text{S}_2\text{N}]^{2-}$ intermediate to form $[\text{HgI}_2\text{S}_2\text{N}]^-$ and yield **5**. The transformation through a five-coordinate intermediate is more likely because Hg can increase its coordination, and the transformation proceeds via an associative mechanism.

Conclusion

Novel mercury(II) thiolate clusters have been synthesized and characterized. A mechanistic pathway for the formation of these clusters through low-coordinate mercury(II) thiolate intermediates is proposed. The intramolecular exchange observed in **4** to **5** is the first for a mercury(II) thiolate, where the ligand exchange is observed in four-coordinate Hg without varying the reaction conditions. This exchange process has been reported earlier but with variable counteranions and varying reaction conditions. This exchange might be useful in understanding the conversion of heteroleptic mercury(II) thiolates to homoleptic mercury(II) thiolates in

(44) Veveris, O.; Bankovskii, Y. A.; Pelne, A. *Latv. PSR Zinat. Akad. Vestis, Kim. Ser.* **1975**, *4*, 451.

(45) Zuka, I.; Bankovskii, Y. A.; Borodkin, Y. G. *Russ. J. Coord. Chem.* **1979**, *5*, 1765.

biological systems. One important conclusion from this work is the structure-directing influence of the halide in these systems, a feature that had not been identified in the previous literature.

Acknowledgment. This work was supported by the University of Kentucky Tracy Farmer Center for the Environment with partial support from the Center for Applied Energy Research Center Fund. NMR instruments used in this research were obtained with funds from the CRIF program

of the National Science Foundation (Grant CHE 997841) and from the Research Challenge Trust Fund of the University of Kentucky.

Supporting Information Available: Syntheses, characterization information, additional figures, extensive tables, thermograms, crystal data, and ^{199}Hg NMR of **1** and **4**. This material is available free of charge via the Internet at <http://www.pubs.acs.org>.

IC060863E